Analysis of barrel structure optimization for a mortar

LIU Qi-feng, ZHAO Han-dong, XIE Jia-qing

(*College of Mechatronic Engineering, North University of China, Taiyuan 030051, China*)

Abstract: Considering the maximum elastic limitation of the used material with newly advanced technology, the study focuses on optimization of a mortar barrel structure by thinning the wall to reduce the weight. Firstly, static analysis of barrel structure parameters is done based on finite element analysis (FEA) method and 3D solid model of the barrel is established based on Unigraphics NX (UG). Secondly, the 3D solid model is simplified and transplanted to ANSYS for barrel wall pressure calculation. Thus, the change curves of the stress exerted on the barrel wall at different locations perpendicular to the axial direction with wall thinning are drawn. By analyzing all possible optimization schemes, the optimal design that enables the barrel to have higher bearing capacity is got. The optimized barrel structure is verified by means of fluid-solid coupling dynamic response analysis. The results show that the static analysis results are closer to real stress conditions than dynamic analysis results. Finally, the barrel weight is reduced by 13% after simulation optimization and the light weight design of the barrel is effective and reliable.

Key words: barrel; finite element analysis (FEA); Unigraphics NX (UG); fluid-solid coupling

CLD number: TJ31 **Document code**: A

Article ID: 1674-8042(2015)03-0258-06 **doi**: 10.3969/j.issn.1674-8042.2015.03.010

As a kind of side arms for infantry, mortars[1] belong to the cannons with fine motility. Barrel, as the most important component of a mortar, plays a prominent role in leading the movement of pellet and exerting initial velocity on the pellet under the pressure of powder gases. Therefore, the performance of the barrel will directly affect the performance of the mortar.

With manpower reduction in actual combats, a single-operated cannon is in a great need, which means that shooting operation only uses a barrel without any riser plate. In this case, light-weight and flexibility of the barrel become quite important. In this paper, barrel structure optimization for the mortar is discussed.

1 Establishment of finite element analysis model

Established by 3D solid modeling software unigraphics NX (UG), an actual computer aided design (CAD) solid model of a mortar barrel is shown in Fig. 1. With the change of wall thickness of the barrel, the quality and capability of the barrel will be influenced and barrel mass M with different wall thickness values can be calculated.

Fig. 1 CAD solid model of a barrel

The material of the barrel is seamless alloy steel, $35CrMnNi_2MoVA$. In the process of shooting, elastic model is chosen as constitutive model of the material because plastic deformation of the barrel can not be allowed. When stimulation results surpass the given yield limit of the material by comparing the barrel stress value with its yield limit, barrel material plastic deformation occurs. Table 1 is the mechanical performance parameters of the barrel material.

Received date: 2015-04-29

Corresponding author: LIU Qi-feng (173563001@qq.com)

Table 1 Material performance parameters

Density (kg/m^3)	Elastic modulus (MPa)	Poisson ratio	Elastic limit (MPa)
7 840	2 070	0.3	1 230

2 Stress analysis by ANSYS[7]

Regardless of the influence of shooting process, variable pressure is exerted on the inner wall alongside the whole barrel, which is based on p-t curve derived from v-t curve (see Fig. 2), which shows the stress and pressure conditions of the barrel.

The established geometric model of the barrel by UG is transplanted into ANSYS Multiphysics. Considering the structural symmetry and loading weight in finite element calculation analysis , only one-fourth of the solid model is selected for a small amount of calculation. A better value is concluded by hexahedral grid partition. The established tube finite element analysis (FEA) model is shown in Fig. 3.

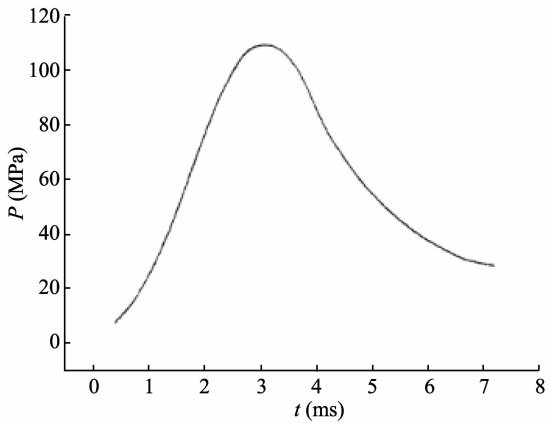

Fig. 2 Velocity-time curve of pellet

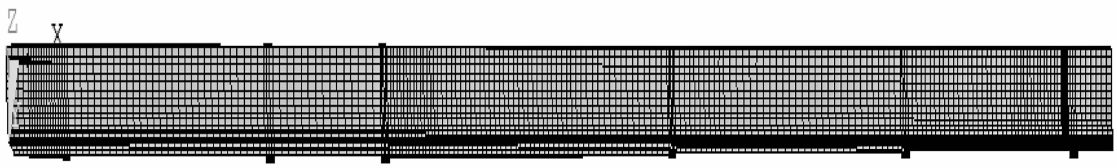

Fig. 3 One-fourth finite element analysis model

According to maximum distortion energy theory (the fourth strength theory)[2-3], the deformation of elastomers produces by external force. Thus, the elastomers hold energy. The energy collected in this way also occurs in the process of loading. They are called strain energy and divided into two kinds: distortional strain energy and volume change energy. The main factor affecting material yield is distortional strain energy density. Material yield occurs on condition that the distortional strain energy density reaches the same density as that under simple tension yield condition.

In a word, the distribution of barrel stress is converted into single-face stress distribution by

$$\sigma_s = \frac{1}{\sqrt{2}} \sqrt{(\sigma_1-\sigma_2)^2+(\sigma_2-\sigma_3)^2+(\sigma_3-\sigma_1)^2}. \quad (1)$$

Then σ_s will be compared with the specified allowable stress.

Perpendicular to the axial direction of the barrel, the inner wall is under different pressure values. The different von Mises stress values on the barrel are measured and analyzed. Table 2 presents the stress values alongside the inner wall of the barrel by calculation. After they are exerted to the corresponding part of the barrel, the final stress nephogram is got, as shown in Fig. 4.

Table 2 Simulation results

Maximum stress (MPa)	Stress at different distances (MPa)							
	200 mm (MPa)	400 mm (MPa)	600 mm (MPa)	800 mm (MPa)	1 000 mm (MPa)	1 200 mm (MPa)	1 400 mm (MPa)	1 500 mm (MPa)
1 228	835	812	795	698	762	662	820	628

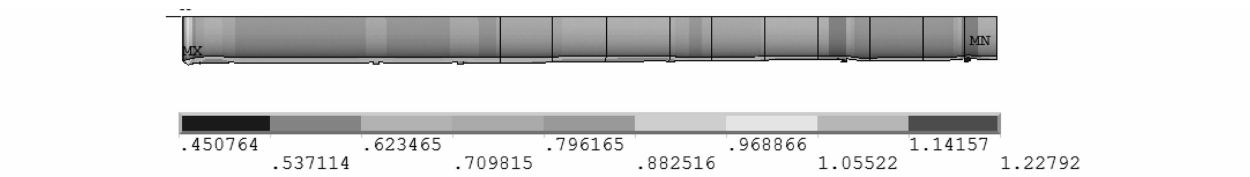

Fig. 4 Stress nephogram of barrel inner wall

The stress curve at different sections of the barrel is shown in Fig. 5. It can be seen that the bottom of the barrel (100—300 mm) receives high stress which is basically even. The muzzle of the barrel (1 300—1 400 mm) suffers high stress and the largest stress can reach up to 1 228 MPa. The ribs on the exterior of the barrel can enhance the strength of the barrel and greatly lower the stress.

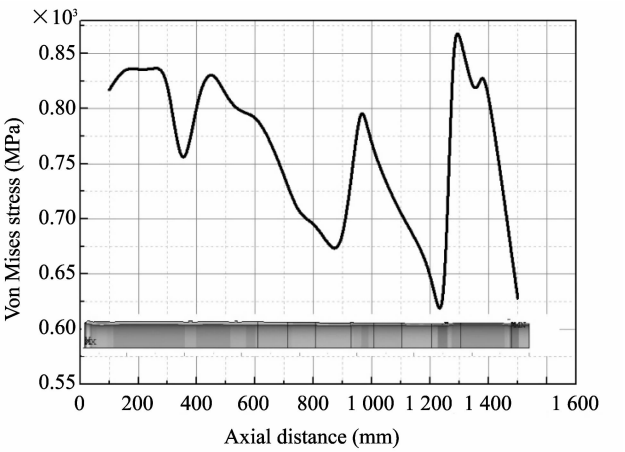

Fig. 5 Stress curve alongside barrel inner wall

3 Estimation of wall thickness reduction of barrel

The thickness of the bottom of the barrel is 10 mm and the thickness of the muzzle is 5 mm[4]. For this reason, a gradually thinning method should be the best choice. Under the circumstance that the inside diameter of the barrel holds 60 mm and the sizes of the ribs on the exterior remain unchanged, the wall thickness is reduced by 0. 25 mm each time. Then the corresponding model is established and the corresponding stress value is got, too. The results are shown in Fig. 6.

By observing the stress nephogram above, it can be found that the bottom of the barrel suffers a sustainable high stress. Because this part is located at the joint of the barrel and there is not a united simulation with other components, the stress of this part is only for a reference without detailed analysis. Furthermore, when the inner wall is under stress, the bottom and the top parts of the barrel receive higher stress, while the middle part receives lower stress. This tendency becomes gradually obvious with the decreasing of the wall thickness of the barrel.

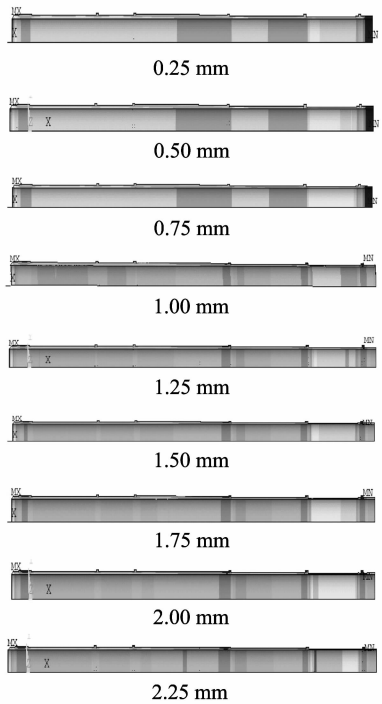

Fig. 6 Stress nephogram of barrel after wall thickness reduced by 0. 25 mm each time

Table 3 illustrates the relationship of barrel weight, barrel stress and wall thickness thinning amount. The maximum stress stands for the largest stress value of the bottom which is only a reference. The 200 mm, 400 mm and so on mean the position to which the stress is exterted and measured from the bottom. The results show that at 1 300 mm and 1 400 mm, the highest stress is received. With the wall thickness decreasing by 1. 5 mm, the stress reaches the elastic limitation.

Conducting curve fitting on the above data, we get several change curves that reveal barrel weight

change law with wall thinning and stress change law at different sections with wall thinning. Details can be seen in Figs. 7—10.

Comparing all the dynamic characteristics mentioned above, we draw a conclusion that when the wall thickness thinning reaches 1.5 mm, the barrel weight is the least and its elastic limitation reaches the largest. Therefore, the barrel performs best.

Table 3 Relation between barrel weight and received thickness-dependent stress at different positions

Reduced thickness (mm)	Weight of barrel (kg)	Maximum stress (MPa)	Stress (MPa)							
			200 mm	400 mm	600 mm	800 mm	1 000 mm	1 200 mm	1 300 mm	1 400 mm
0.25	41.487 7	1 309.27	858.03	851.58	812.05	705.10	802.66	691.63	923.00	869.18
0.50	40.194 6	1 347.04	877.08	871.38	824.87	724.99	825.71	715.82	972.78	914.14
0.75	38.859 7	1 387.01	897.61	891.06	842.54	737.90	856.93	743.54	1 021.20	962.61
1.00	37.577 5	1 429.57	919.11	913.25	862.15	755.60	892.62	770.15	1 082.50	1 018.00
1.25	36.300 1	1 474.78	941.82	936.22	882.11	774.54	924.31	801.08	1 152.20	1 085.00
1.50	35.027 3	1 522.93	965.87	960.58	902.47	793.78	962.29	836.34	1 230.40	1 155.40
1.75	33.759 3	1 574.27	991.39	986.48	925.11	817.74	1 004.50	871.35	1 318.10	1 243.30
2.00	32.496 0	1 629.13	1 018.50	1 014.00	953.12	839.73	1 053.40	913.50	1 421.60	1 337.30
2.25	31.237 5	1 687.83	1 047.40	1 045.70	978.25	863.10	1 101.60	955.66	1 544.40	1 459.00

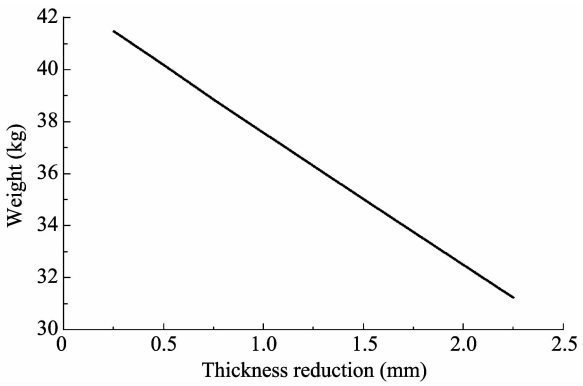

Fig. 7 Weight at different thickness amounts

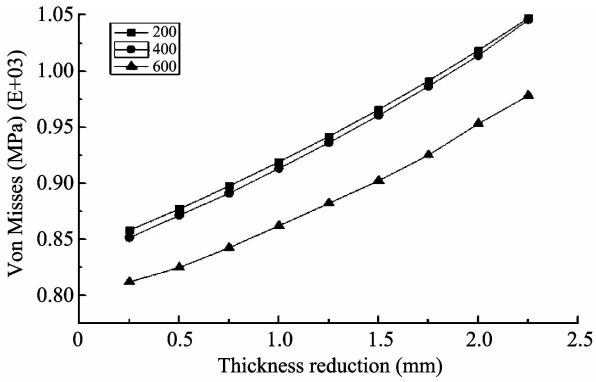

Fig. 8 Stress at different thickness reduction amounts at sections of 800, 1 000 and 1 200 mm

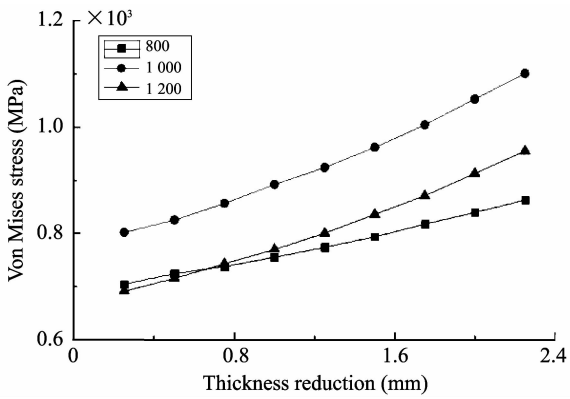

Fig. 9 Stress at different thickness reduction amounts at sections of 200, 400 and 600 mm

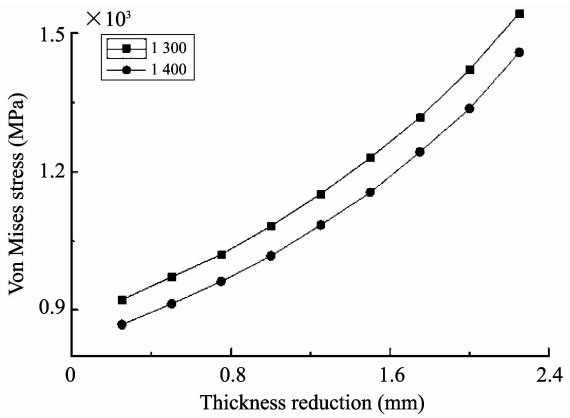

Fig. 10 Stress at different thickness reduction amounts at sections of 1 300 and 1 400 mm

4 Verification

Interior ballistic model studies the shooting phenomenon inside the barrel bore. This paper adopts the classical interior model[4], and the following hypotheses should be obeyed:

1) Propellant combustion should obey the geomet-

ric burning law;

2) Propellant combustion gas should obey the Nobel Abel equation;

3) Mechanical work during the interior ballistic process should be proportional to $\frac{1}{2}mv^2$;

4) Airflow inside the barrel conforms to Lagrange hypothesis which also assumes the grains burn under an average pressure and obey the combustion velocity law.

Based on the above hypotheses, the basic equations of the cannon interior ballistics are given as[6]

$$\begin{cases} \psi = \chi Z(1+\lambda Z+\mu Z^2),\ 0 \leqslant Z \leqslant 1, \\ \dfrac{dZ}{dt} = \dfrac{p^n}{I_b},\ I_b = \dfrac{e_1}{u_1}, \\ \varphi m \dfrac{dv}{dt} = Sp, \\ \dfrac{dl}{dt} = v, \\ Sp(l_\psi = l) = f\omega\psi - \dfrac{\theta}{2}\varphi m v^2, \\ l_\psi = l_0\left[1 - \dfrac{\Delta}{\rho_p} - \Delta(\alpha - \dfrac{1}{\rho_p})\psi\right], \end{cases} \tag{2}$$

where ψ is the burnout percentage of a gunpowder; e_1, the arc thickness; λ, χ and μ are the shapevolumes; Z is the relevant burnout thickness; u_1, the burning rate; P, average pressure; φ, the secondary powder calculation ratio; n, the burning rate exponent; m, the pellet mass; V, the pellet kinematic velocity; S, the bore sectional area; l, the pellet stroke length; l_ψ, the necking length of powder chamber free volume; f, the impetus; ω, the explosive load; θ, the gunpowder thermal parameter; Δ, the gunpowder loading density.

Various methods are adopted to obtain the gun pressure P values on different parts alongside the barrel, thus the mortar interior ballistic verification can be achieved. Specific methods include the interior ballistic mathematical model from Eq. (2), Runge Kutta method and FEA method.

Fluid structure interaction dynamic analysis of the light weighted barrel is conducted by using the interior ballistic data[7]. Research findings of the barrel deformation under higher gun pressure are tested if they turn out the ideal conditions from the dynamics aspect. Fig. 11 is about received stress of the barrel.

Fig. 11 Stress of a working mortar

Table 4 lists the different received stresses alongside the barrel after shooting.

It can be concluded from Table 4 that there is only 5.6% difference between simulation results and optimized results, which can be considered as the different applications of arithmetic. Therefore, this light weight result can be trusted and used for future experiments.

Table 4 Stress at axial sections when a shell shooting

Stress (MPa)								
Max	200 mm	400 mm	600 mm	800 mm	1 000 mm	1 200 mm	1 300 mm	1 400 mm
1 493.8	1 012.2	905.9	834.2	728.7	885.4	753.1	1 160.8	1 082.2

5 Analysis

First, ANSYS statics simulation method is provided as a basic research background[8]. The variable pressure is applied to the inner wall of the barrel perpendicula to the axial direction. The research focuses on the relationship between thickness thinning amount of mortar barrel and changes of wall stress. Then a model is built with a constant 0.25 mm wall

thickness reduction of the barrel, and the stress curve of the barrel is got. Dynamic simulation verification by fluid-solid coupling is finally used for the barrel model. It shows that ANSYS statics simulation method acts as the most effective method, which suggests itself be helpful to the optimization design of a mortar.

6 Conclusions

1) Without assembly at the bottom of the barrel, stress value reaches 1 228 MPa, while with a constantly decreasing thickness, stress value increases at the same time, which provides unreliable results in this research.

2) The high gun pressure section at 600 mm receives sustainable stress with constant thickness reduction. When the thickness reduction reaches 2.25 mm, the stress does not reach elastic limitation.

3) When the thickness reduction reaches 1.5 mm and weight decreases 6.5 kg which is a decrease of 15.2% in barrel mass, stress at 1 300 mm section firstly reaches the elastic limitation.

4) Ribs on the exterior have an outstanding ability to enhance the strength. Thus they are applied to weak sections. We get a quick stress value of relevant simulation calculation;

5) The data in the fluid structure interaction appear as a smaller one than that in the optimization. Besides, the bottom receives the highest stress where the projectile is launched. Gun pressure constantly decreases with projectile moving. These signs manifest that the optimization is more reasonable and safer in an actual application, therefore it plays a helpful role in the future research.

References

[1] ZHAO Xi-fa, LI Zhi-long. Mortars Gossip. Samll Arms, 2008, (4): 9-11.

[2] SU Yi-lin. Mechanics of materials (2nd edition. Beijing: Higher Education Press, 1987: 195-196.

[3] Pisarenko Ke Γ C. Material mechanical manual. Beijing: China Building Industry Press, 1981: 192-193.

[4] DONG Ming, WANG Ting. Mortar barrel temperature stress analysis based on ANSYS. Mechanical Engineering and Automation, 2014, (4): 3-4.

[5] BAO Ting-yu, QIU Wen-jian. Internal ballistics. Beijing: Beijing Institute of Technology Press, 1995.

[6] Geskin é S, Petrenko O P, Rusanova O A, et al. Strength analysis and optimization of the barrel nozzle of a powder water cannon. Strength of Materials, 2006, (2): 23-25.

[7] MA Chi-cheng, ZHENG Xi-nong, LUO Ya-jun, et al. Dynamic responses for a fluid-structure coupling system with variable mass in a tank of spacecraft. Journal of Aerospace, 2015, (3): 737-740.

[8] CHEN Wei-dong, YU Yan-chun, ZHANG Feng-chao, et al. Static stochastic analysis of entity structure based on finite volume method. Journal of Harbin Engineering University, 2015, (7): 1.

某迫击炮身管结构优化分析

刘麒峰，赵捍东，解加庆

（中北大学 机电工程学院，山西 太原 030051）

摘　要： 考虑采用新型工艺后材料最大弹性极限，研究了某迫击炮身管壁厚减薄的结构优化方法。首先，采用有限元方法进行静态分析，通过三维软件 UG 建立了身管实体模型。对身管结构进行合理简化后，导入到 ANSYS 中进行膛压分析计算，得到了身管不同位置管壁所受应力随壁厚减薄的变化曲线。综合分析各种壁厚减薄方案，得到了身管承载性能最优的方案，并采用流固耦合动态响应加以验证。结果表明，静态分析结果较动态分析结果更接近真实受力状况。最终，迫击炮身管结构重量经仿真优化后可减轻 13%，因而，该身管轻量化方法有效而可靠。

关键词： 身管；有限元分析；UG；流固耦合

引用格式： LIU Qi-feng, ZHAO Han-dong, XIE Jia-qing. Analysis of barrel structure optimization for a mortar. Journal of Measurement Science and Instrumentation, 2015, 6(3): 258-263. [doi: 10.3969/j. issn. 1674-8042. 2015. 03. 010]